Supplementary Materials

Investigation of the optical and excitonic properties of the visible-light driven photocatalytic $BiVO_4$ material

Tilak Das[1], Xavier Rocquefelte[1,2], Robert Laskowski[3], Luc Lajaunie[1,4], Stéphane Jobic[1], Peter Blaha[5] and Karlheinz Schwarz[5]

[1]*Institut des Matériaux Jean Rouxel, Université de Nantes, CNRS, Boîte Postale 32229, 44322 NANTES Cedex 3, France.*

[2]*Institut des Sciences Chimiques de Rennes, UMR 6226 CNRS, Université de Rennes 1, 35042 Rennes Cedex, France.*

[3]*Institute of High Performance Computing, 1Fusionopolis Way, #16-16 Connexis North, Singapore 138632.*

[4]*Laboratorio de Microscopías Avanzadas, Instituto de Nanociencia de Aragón, Universidad de Zaragoza, 50018 Zaragoza, Spain.*

[5]*Institute of Materials Chemistry, Vienna University of Technology, Getreidemarkt 9/165-TC, A-1060 Vienna, Austria.*

Structural description

Table S1. The Bi-V distances and corresponding Bi-O-V angles in S_M- and Z_T-$BiVO_4$ phases. The colors correspond to the ones used in Figs. 1c and 1d.

Phase	Orientation	Bi-V distances (Å)	Bi-O-V angles (°)	1st bright exciton
S_M-$BiVO_4$	in-plane	3.65 (×2) – red 3.62 (×2) – red	118.9 (×2) 121.5 (×2)	2.41
	out-of-plane	4.03 (×2) – green 3.76 (×2) – orange	136.7 (×2) 131.1 (×2)	2.88
Z_T-$BiVO_4$	in-plane	4.00 (×4) – green	152.9 (×4)	2.88
	out-of-plane	3.29 (×2) – red	99.6 (×2)	2.79

EELS spectroscopy : Local Field Effects

LFE arises in inhomogeneous periodic crystals where the individual dipoles of the system respond to an induced local-field by the other dipoles of the system and/or by an external field[1]. Figure S1 shows the loss functions along x, y and z for the monoclinic phase and along x and z for the tetragonal phase. The blue solid lines in Figure S1 are our calculated data without inclusion of the LFE correction and red solid lines show the results including this correction via the random phase approximation (RPA). LFE strongly influence the V-$M_{2,3}$ edges (3p(V) → 3d(V) transition) of S_M- and Z_T -$BiVO_4$ in the 40-50 eV energy range of the dielectric functions. In all directions, taking into account LFE strongly decreases the intensity of the edges and shifts them towards higher energies, leading to a better agreement with the experiments. A similar influence of LFE on semi-core states has already been observed on other oxides such as TiO_2, MoO_3 and NiO.[2,3,4] To a lesser extent, LFE also influences the Bi-$O_{4,5}$ edges (5d(Bi) → 5f(Bi) transition), by reducing their width and shifting them to higher energies. In contrast, on the low-energy range of the spectra, the LFE have little impact on the two structures A and B of the energy loss function in both S_M- and Z_T -$BiVO_4$.

The experimental measurements have been carried out with a low collection angle, allowing a direct comparison between the recorded and calculated loss-functions at zero momentum transfer (q=0). Due to the nearly isotropic nature of the loss-function of S_M-$BiVO_4$, the experimental curve is compared to the average calculated LFE corrected loss-function (top panel of Fig. S2a). In the central panel the data of ε_1 and ε_2 are enhanced five times with respect to the bottom panel. In a similar strategy, the loss-function of Z_T-$BiVO_4$, has been recorded along the [1 1 0] zone axis (see top panel of Fig. S2b). For this phase the anisotropy of the loss-function is not negligible. For comparison with experiments, we have used EEL spectra collected along the z-axis, and the Im ($-1/\varepsilon_{zz}$) theoretical data.

Let's now explain the origin of the different features of the loss-function of S_M-$BiVO_4$. At about 11 eV, the structure A corresponds to a zero of ε_1 (with a positive slope) and to no particular feature in ε_2. This is characteristic of a plasmon (collective mode). On the other hand, at about 20 eV, structure B is due to an absorption peak in ε_2 associated with an oscillation in ε_1. This is characteristic of an inter-band transition. Because the energy loss function is equal to $Im(-1/\varepsilon) = \varepsilon_2/(\varepsilon_1^2 + \varepsilon_2^2)$, the inter-band

transitions in ε_2 induce a peak in the loss-function that is shifted towards the higher energies[1]. Finally, mainly two others structures are observed, at about 30 and 50 eV, which correspond to semi-core Bi-$O_{4;5}$ and V-$M_{2;3}$ edges, respectively. Similar statements regarding the interpretation of the energy loss function can be made for Z_T-$BiVO_4$.

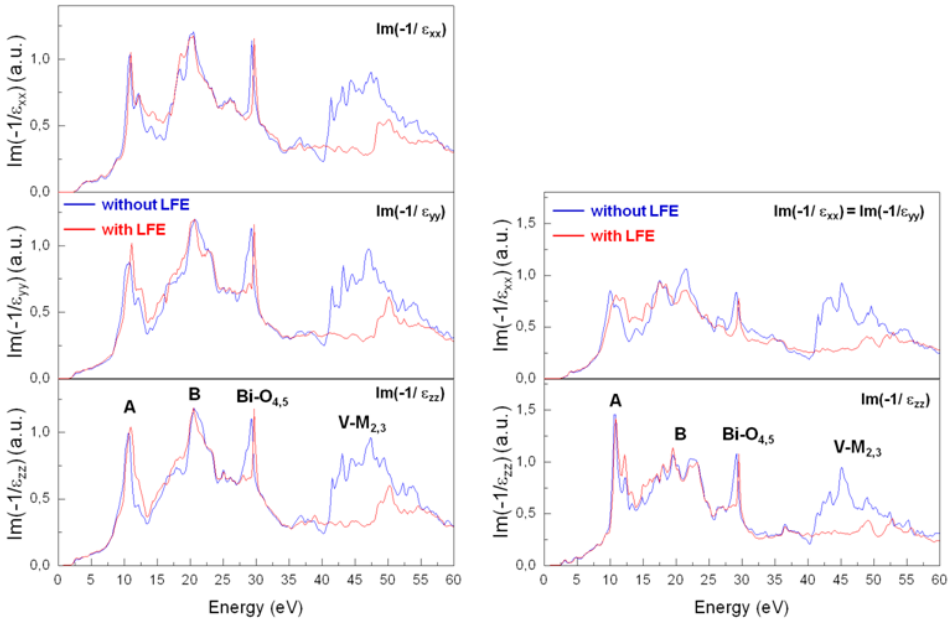

Figure S1. Influence of the inclusion of the local-field effects on the calculation of the energy-loss functions of S_M-$BiVO_4$ and Z_T-$BiVO_4$.

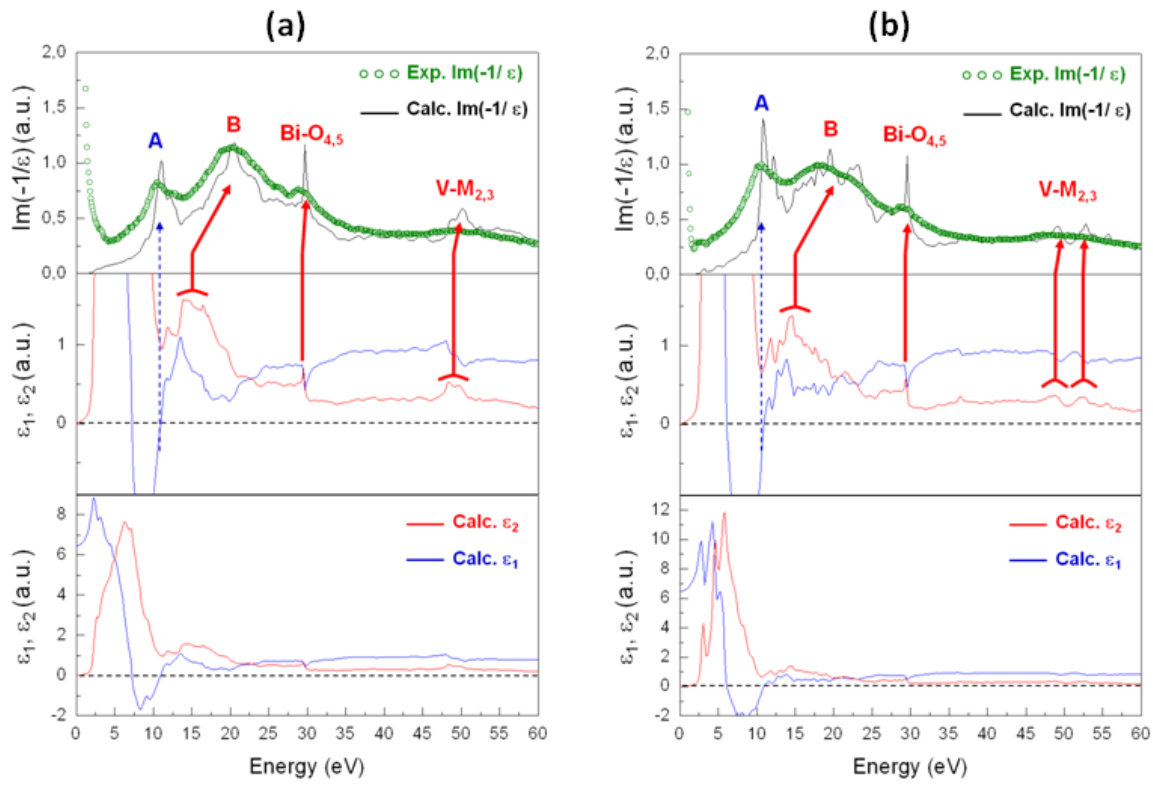

Figure S2. Energy-loss (Im(-1/ε)) and dielectric (ε_1, ε_2) functions of S_M-$BiVO_4$ (a) and Z_T-$BiVO_4$ (b) with local-field effects taken into account. The experimental VEELS spectra of S_M- and Z_T-$BiVO_4$ have been recorded along the [9 11 4] and [1 1 0] zone axes, respectively. For comparison, the calculated quantities correspond to an average of the polarizations along x, y and z for S_M-$BiVO_4$ and a polarization along z for Z_T-$BiVO_4$.

Density of states of $BiVO_4$

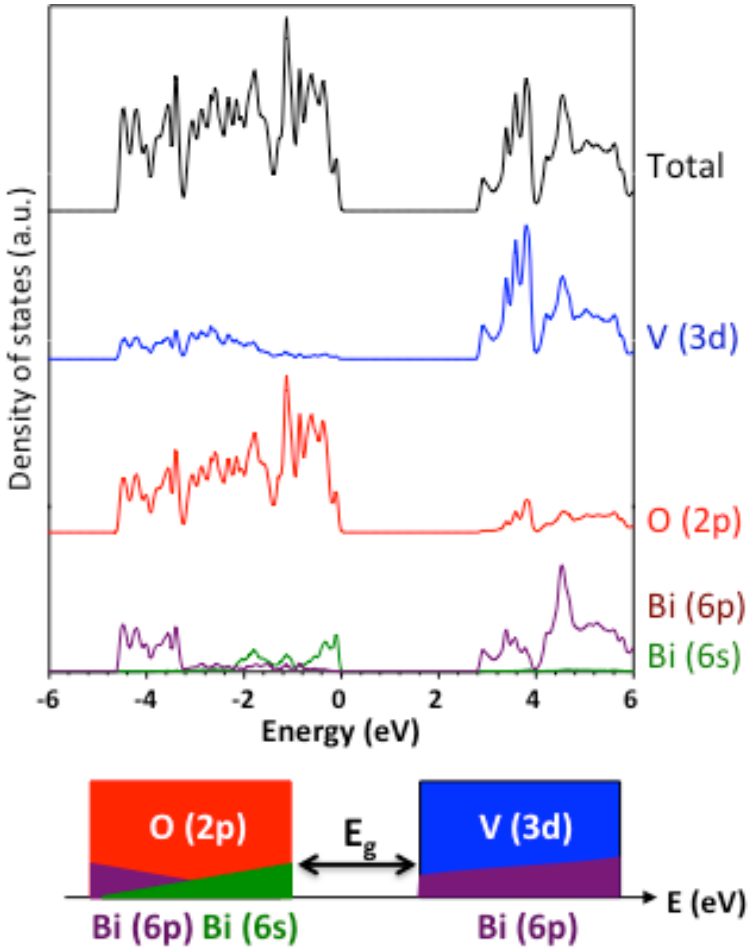

Figure S3. Total and partial densities of states of Z_T-$BiVO_4$ using GGA calculations. The partial densities of states of Bi(6s) and Bi(6p) have been multiplied by a scaling factor in order to facilitate the chemical bond analysis. A scheme (bottom) is given which summarizes the nature of the valence and conduction bands. It allows to understand the excitonic distribution with the photo-hole mainly on O(2p) and the photo-electron mainly on V(3d) states., but it also explain the significant contribution of Bi(6s) and Bi(6p) states. A similar scheme is found for S_M-$BiVO_4$.

BSE calculations

Table S2. S_M-$BiVO_4$

Exciton	*E (eV))*	*Osc.x*	*Osc.y*	*Osc.z*	E_b *(eV)*
1	2.41	**571**	**43**	0	0.384
2	2.47	**181**	**271**	0	0.418
3	2.49	**94**	**541**	0	0.439
5	2.54	**18**	**7**	0	0.185
6	2.54	**1**	**23**	0	0.266
7	2.54	**15**	0	0	0.154
15	2.58	**20**	0	0	0.138
17	2.59	**26**	**1**	0	0.162
27	2.62	**7**	0	0	0.123
30	2.62	**7**	0	0	0.117
35	2.63	**9**	0	0	0.112
36	2.64	**7**	0	0	0.112
38	2.64	**30**	0	0	0.139
247	2.79	**6**	0	0	0.113
396	2.85	0	**5**	0	0.111
470	2.88	0	0	**7**	0.104

Table S3. Z_T-$BiVO_4$

Exciton	*E (eV))*	*Osc.x*	*Osc.y*	*Osc.z*	E_b *(eV)*
3	2.79	2	5	**772**	0.610
4	2.88	**150**	**105**	15	0.742
5	2.88	**117**	**155**	1	0.763
9	3.03	0	1	**16**	0.239
11	3.06	**5**	**3**	0	0.230
134	3.20	**19**	0	0	0.226
135	3.20	1	**20**	0	0.233
138	3.20	**12**	**9**	0	0.233

Table S4. Anatase-TiO_2

Exciton	*E (eV))*	*Osc.x*	*Osc.y*	*Osc.z*	E_b *(eV)*
1	3.84	**187**	0	0	0.608
2	3.84	0	**187**	0	0.608
9	4.03	**23**	0	0	0.223
10	4.03	0	**23**	0	0.223

19	4.11	**31**	0	0	0.252
20	4.11	0	**31**	0	0.252
23	4.17	**29**	0	0	0.239
24	4.17	0	**29**	0	0.239
28	4.24	0	0	**272**	0.637
42	4.29	0	0	**245**	0.594
68	4.34	**87**	0	0	0.987
69	4.34	0	**87**	0	0.989
181	4.56	**130**	0	0	0.963
182	4.56	0	**129**	0	0.963
183	4.57	**35**	0	0	0.248
184	4.57	0	**35**	0	0.248
185	4.58	0	0	**30**	0.451
199	4.60	**24**	0	0	0.307
200	4.60	0	**24**	0	0.307

Table S5. Rutile-TiO_2

Exciton	*E (eV))*	*Osc.x*	*Osc.y*	*Osc.z*	*E_b (eV)*
3	*3.54*	*1*	*1*	*0*	*0.243*
4	*3.54*	*1*	*1*	*0*	*0.243*
7	*3.62*	*0.5*	*0.4*	*0*	*0.140*
8	*3.62*	*0.4*	*0.5*	*0*	*0.140*
14	*3.72*	*3.0*	*4.6*	*0*	*0.267*
15	*3.72*	*4.6*	*3.0*	*0*	*0.267*
19	*3.79*	*0.3*	*0.1*	*0*	*0.175*
20	*3.79*	*0.1*	*0.3*	*0*	*0.175*
24	3.82	0	0	**165**	0.605
59	3.97	0	0	**37**	0.270
60	3.97	**65**	**104**	0	0.488
61	3.97	**104**	**65**	0	0.489
72	4.03	0	0	**120**	0.359
80	4.04	**43**	**4**	0	0.273
81	4.04	**4**	**43**	0	0.273
84	4.05	**26**	**9**	0	0.266
85	4.05	**9**	**26**	0	0.266
86	4.05	0	0	**101**	0.361
107	4.08	**32**	**23**	0	0.302
108	4.08	**23**	**32**	0	0.302
117	4.09	0	0	**73**	0.286
197	4.19	0	0	**43**	0.232
215	4.22	0	0	**77**	0.262
295	4.31	0	0	**22**	0.235
460	4.40	0	0	**72**	0.255

Summary of the main results

Table S6. Optical and excitonic properties of the four compounds.

	S_M-$BiVO_4$	Z_T-$BiVO_4$	Ana-TiO_2	Rut-TiO_2
Band gap	Indirect	Direct	Indirect	Direct
1st exciton	Bright	Dark	Bright	Dark
1st exciton polarization	⊥ c	// c	⊥ c	// c
Number of bright excitons among the first fifties	12	5	10	1

[1] Raether, H. Excitations of Plasmons and Interband Transitions by Electrons *Springer Tracts in Modern Physics* **1980**, 88, ISBN – 978-3-540-09677-1(print).

[2] Vast, N.; Reining, L.; Olevano, V.; Schattschneider, P.; Jouffrey, B. Local Field Effects in the Electron Energy Loss Spectra of Rutile TiO_2 *Phys. Rev. Lett.* **2002**, 88, 037601.

[3] Aryasetiawan, F.; Gunnarsson, O.; Knupfer, M.; Fink, J. Local-field effects in NiO and Ni *Phys. Rev. B* **1994**, 50, 7311.

[4] Lajaunie, L.; Boucher, F.; Dessapt, R.; Moreau, P. Strong anisotropic influence of local-field effects on the dielectric response α-MoO_3 *Phys. Rev. B* **2013**, 88, 115141.